HUMAN GENE THERAPY 22:189–196 (February 2011)

DOI: 10.1089/hum.2010.098

Noninvasive Repetitive Imaging of Somatostatin Receptor 2 Gene Transfer with Positron Emission Tomography

Gabriella Cotugno,[1,2*] Michela Aurilio,[3*] Patrizia Annunziata,[1,2] Anita Capalbo,[1,2] Armida Faella,[1] Valentina Rinaldi,[3] Caterina Strisciuglio,[1,2] Maurizio Di Tommaso,[1] Luigi Aloj,[3] and Alberto Auricchio[1,2]

Abstract

Noninvasive *in vivo* imaging of gene expression is desirable to monitor gene transfer in both animal models and humans. Reporter transgenes with low endogenous expression levels are instrumental to this end. The human somatostatin receptor 2 (hSSTR2) has low expression levels in a variety of tissues, including muscle and liver. We tested the possibility of noninvasively and quantitatively monitoring hSSTR2 transgene expression, following adeno-associated viral (AAV) vector-mediated gene delivery to murine muscle and liver by positron emission tomography (PET) using ^{68}gallium-DOTA-Tyr^3-Thr^8-octreotate (^{68}Ga-DOTATATE) as a highly specific SSTR2 ligand. Repetitive PET imaging showed hSSTR2 signal up to 6 months, which corresponds to the last time point of the analysis, after gene delivery in both transduced tissues. The levels of tracer accumulation measured in muscle and liver after gene delivery were significantly higher than in control tissues and correlated with the doses of AAV vector administered. As repetitive, quantitative, noninvasive imaging of AAV-mediated SSTR2 gene transfer to muscle and liver is feasible and efficient using PET, we propose this system to monitor the expression of therapeutic genes coexpressed with SSTR2.

Introduction

Advances in gene therapy over the last few years have shown the potential to obtain safe, long-term, tissue-specific expression of therapeutic proteins via viral- or nonviral-mediated transduction of selected target cells (Brunetti-Pierri and Auricchio, 2010). However, for both efficacy and safety concerns, monitoring transgene expression in time and space might be required to ensure controlled and effective delivery of the desired gene to target cells and avoid expression in nontarget locations.

Various markers have been used for this purpose, consisting of either proteins secreted in the bloodstream, whose concentration can be measured in the serum, or cellular proteins, whose presence can be detected histologically [β-galactosidase or enhanced green fluorescent protein (eGFP)] (Ray *et al.*, 2001). In the former case, measurable circulating levels of the secreted marker protein prove transduction, but fail to localize the transduced tissue. In the latter case, an invasive tissue biopsy is required to assess gene expression: in a recent clinical trial testing the efficacy and safety of adeno-associated viral (AAV) vector-mediated gene transfer to the muscle of hemophilia B patients, multi-year therapeutic gene expression was documented by immunohistochemical analysis of factor IX expression in patient muscle biopsies (Manno *et al.*, 2003; Jiang *et al.*, 2006).

In vivo imaging techniques have been developed that allow noninvasive, repeated monitoring of reporter gene expression, thus avoiding the requirement of tissue sampling for histological analysis of transgene expression (Ray *et al.*, 2001; Gilad *et al.*, 2008; Min and Gambhir, 2008). Optical reporter genes, such as firefly luciferase or eGFP, are currently being used to monitor gene expression *in vivo* in animal models (Ray *et al.*, 2001; Min and Gambhir, 2008). Despite the advantage of low signal background and low cost (Min and Gambhir, 2008), these techniques show limited resolution especially in deep tissues and, therefore, can not be extended to human applications (Min and Gambhir, 2008). In addition, the nonhuman origin of such reporter genes could likely produce in patients an immune response ablating the transduced cells.

Radiotracer imaging techniques, such as positron emission tomography (PET) and single-photon emission computerized tomography (SPECT), allow the detailed location, magnitude, and time variation of the reporter gene expression to be monitored with high sensitivity (Gambhir *et al.*,

[1]Telethon Institute of Genetics and Medicine (TIGEM), 80131 Naples, Italy.
[2]Medical Genetics, Department of Pediatrics, "Federico II" University, 80131 Naples, Italy.
[3]Department of Nuclear Medicine, Istituto Nazionale Tumori, Fondazione "G. Pascale," 80131 Naples, Italy.
*G.C. and M.A. contributed equally to this work.

2000a; Ray *et al.*, 2001; Min and Gambhir, 2008), with PET allowing higher spatial resolution and easier quantification of radiotracer levels than SPECT (Gambhir *et al.*, 2000b). In addition, PET analysis is routinely performed in human patients to monitor tumor progression (Kayani *et al.*, 2008), thus allowing the use of PET reporter genes to be scaled up for human applications.

Several PET reporter genes have been used to efficiently image gene transfer directed to different tissues and tumors in animal models. These include the herpes simplex virus 1 thymidine kinase (HSV1-tk) (Gambhir *et al.*, 2000a; Ray *et al.*, 2001), the dopamine 2 receptor (D2R) (MacLaren *et al.*, 1999; Ray *et al.*, 2001), the sodium iodide symporter (NIS) (Groot-Wassink *et al.*, 2004), and the somatostatin (SST) receptor 2 (SSTR2) (Zinn *et al.*, 2000, 2002; Kundra *et al.*, 2002; Zinn and Chaudhuri, 2002; Rogers *et al.*, 2003, 2005; Singh *et al.*, 2009). For each of these reporters, radiotracers have been developed that are bound to or converted by the reporter transgene product (Min and Gambhir, 2008).

SSTR2 is a member of the SSTR G-protein–coupled receptor family, which includes five separate membrane receptor genes (SSTR1 to SSTR5); SST binding to SSTRs produces an inhibitory signal, which results in antimitotic action as well as inhibition of secretory processes (Hofland and Lamberts, 1996). The SSTR subtypes are widely distributed with varying tissue levels in the brain, gastrointestinal tract, pancreas, kidney, and spleen (Yamada *et al.*, 1992; Hoyer *et al.*, 1995). In addition, most neuroendocrine tumors (NET) originating from SST target tissues have conserved expression of SSTRs (Hofland and Lamberts, 1996). SST analogues radiolabeled with positron emitters and with affinity to SSTR2, such as ^{68}gallium-DOTA-Tyr^{3}-Thr^{8}-octreotate (^{68}Ga-DOTATATE) and ^{68}gallium-DOTA-D-Phe^{1}-Tyr^{3}-octreotide (^{68}Ga-DOTATOC) (Froidevaux *et al.*, 2002), are currently used in clinical settings for PET imaging of NETs (Win *et al.*, 2007; Miederer *et al.*, 2009) and show good safety profiles.

Among the described PET reporter genes, SSTR2 presents several advantages that make it attractive as a reporter for *in vivo* imaging of transgene expression: (i) Its human origin should avoid potential immune responses developed against nonhuman transgenes, such as the HSV1-tk. (ii) As opposed to intracellular reporter genes (*i.e.*, tk), the use of a membrane receptor avoids the requirement for the radioactive probe to cross the cell membrane. This could reduce the potential variations in PET signal that might be related to differences in intracellular entry of the reporter probe in different cells. (iii) The availability of SST analogues approved for human use is important when considering the application of SSTR2-based imaging techniques for use in patients. (iv) SST analogues are excreted mostly in urine (Froidevaux *et al.*, 2002), avoiding the problems encountered with probes that have hepatobiliary excretion and long residence times in the gastrointestinal tract, such as those used for D2R, which make imaging target structures in the abdomen challenging (Herzog *et al.*, 1990; Min and Gambhir, 2008). (v) Human SSTR2 (hSSTR2) signaling exerts an inhibitory action on the proliferation of target cells, and thus its expression should not lead to increased cell proliferation. (vi) Finally, the SSTR2 coding sequence is relatively short (1,110 bp; GenBank: AY236542.1), allowing the generation of bicistronic vectors encoding for both the SSTR2 reporter and a desired therapeutic transgene even in gene therapy vectors with limited cargo capacity, such as AAV.

To date, PET or gamma camera imaging of hSSTR2 has been obtained in animal models bearing xenograft SSTR2-expressing tumors (Zinn *et al.*, 2000, 2002; Kundra *et al.*, 2002; Rogers *et al.*, 2002, 2003, 2005). In addition, gamma camera imaging of SSTR2 expression in the liver has been achieved following delivery with first-generation adenoviral vectors, known to result in short-term transgene expression (Rogers *et al.*, 2003).

Given the SSTR2 potential as a reporter for *in vivo* imaging of gene transfer, its utility in imaging long-term transduction in nontumoral tissues should be investigated in detail. To this end, AAV vectors represent powerful tools for gene transfer given their ability to efficiently and safely transduce various tissues, resulting in long-term transgene expression (Brunetti-Pierri and Auricchio, 2010). Several AAV vector serotypes exist with different tissue tropism (Brunetti-Pierri and Auricchio, 2010), allowing efficient targeted transduction of desired tissues. Most importantly, the safety and efficacy of AAV-mediated gene transfer are being evaluated in humans, and initial results appear very promising (Brunetti-Pierri and Auricchio, 2010).

Here we have exploited both the potential of hSSTR2 as PET reporter gene and the longevity of transgene expression obtained by AAV vectors *in vivo* to quantitatively, non-invasively, and repetitively monitor gene expression in the murine muscle and liver, two crucial targets for gene therapy.

Materials and Methods

Vector construction and production

The pCL-SSTR2 plasmid, containing the hSSRT2a coding sequence (cds; GenBank: AY236542.1) was purchased from UMR cDNA Resource Center, University of Missouri–Rolla (Rolla, MO).

pAAV2.1-CMV-hSSTR2 and pAAV2.1-TBG-hSSTR2 plasmids were produced as follows: The hSSTR2 cds was PCR-amplified from pCL-SSTR2 using the following primers: forward, aattgcggccgcatggacatggcggatgag, and reverse, tata tggatcctcagatactggtttggagg, containing the *Not*I and *Bam*HI restriction sites, respectively. The PCR product was inserted in the pCR Topo 2.1 vector (Invitrogen Corp., Carlsbad, CA), as suggested by the manufacturer, and digested with *Not*I and *Bam*HI (Roche, Basel, Switzerland). hSSTR2 was then cloned into pAAV2.1-TBG-eGFP and pAAV2.1-CMV-eGFP plasmids (Auricchio *et al.*, 2001) previously digested with the same enzymes. The pAAV2.1-TBG-lacZ plasmid (Auricchio *et al.*, 2001) was also used for recombinant AAV production.

Recombinant AAV vectors were produced by triple transfection of 293 cells and purified by CsCl gradients (Xiao *et al.*, 1999). Physical titers of the viral preparations [genome copies (gc) per milliliter] were determined by real time PCR (PerkinElmer, Foster City, CA) (Gao *et al.*, 2000).

Cell culture conditions and AAV transduction

HEK293 cells were grown in Dulbecco's modified Eagle medium (DMEM; Celbio, Milan, Italy) supplemented with 10% fetal bovine serum (FBS; GIBCO, Invitrogen) and penicillin (10 U/ml)–streptomycin (10 μg/ml)–amphotericin B (0.25 μg/ml; Invitrogen). For infection with AAV, cells were incubated in serum-free DMEM and infected with AAV2/1-CMV-hSSTR2 at the multiplicity of infection (MOI) reported

in Fig. 1B, for 2 hr at 37°C. Then complete DMEM medium was added to the cells. Forty-eight hours later, infected cells were either fixed in 4% paraformaldehyde (PFA) for anti-hSSTR2 immunofluorescence or collected for *in vitro* binding assays. Fluorescence intensity in pictures from infected and control cells was quantified by the ImageJ 1.38x software (http://rsb.info.nih.gov/ij/). Results were analyzed for correlation with the AAV vector dose used to infect the cells and the extent of ^{68}Ga-DOTATATE binding.

Mouse models, vector administration, PET analysis, and tissue collection

Adult 1-month-old C57bl/6 mice and BalbC nude (nu/nu) mice were purchased from Harlan Italy Srl (S. Pietro al Natisone, Udine, Italy). AAV2/8-TBG-hSSTR2 vectors were injected in the tail vein, and AAV2/1-CMV-hSSTR2 vectors were injected in the right gastrocnemius. The vector doses used are reported below under Results and Discussion. One, 3, and 6 months after vector administration, 1–6 MBq of ^{68}Ga-DOTATATE was injected into the tail vein of treated and control mice. After 10 min, mice were anesthetized with 2,2,2-tribromoethanol (Avertin; Sigma-Aldrich, St. Louis, MO) and subjected to PET analysis. For visual localization of tracer binding, a clinical PET-computerized tomography (PET-CT) scanner was used (DST 600; General Electric, Fairfield, CT). For quantitative measurements of tracer uptake, animals were analyzed in a SIEMENS ECAT47 clinical PET scanner in two-dimensional mode with measured attenuation correction (Siemens, Erlangen, Germany). Quantitative evaluation for all PET scans was performed using ESOFT software (version 5.0.3; Siemens). A semiautomatic three-dimensional volume of interest (VOI) drawing tool was used. A rough area was manually drawn around the tissue of interest, and the region was subsequently automatically contoured based on a fixed threshold value. The average standardized uptake value (SUV) and the apparent VOI were recorded for the liver and muscle regions. These values were converted to percentage of injected dose per gram (%ID/g) normalized for a 20-g mouse. The %ID/g multiplied by the VOI measured in milliliters (%ID/g×V) was used for comparison of tracer accumulation. After the last time point, animals were sacrificed, and tissues were collected, fixed in 4% PFA, and embedded in OCT compound (Kaltek, Padova, Italy) for anti-hSSTR2 immunofluorescence analysis. Due to their immunodepressed condition, some of the BalbC nude (nu/nu) mice died before the 6-month time point, presumably because they were housed in a conventional facility (Centro di Biotecnologie, "AORN Antonio Cardarelli," Naples, Italy).

In vitro *^{68}Ga-DOTATATE binding assays*

AAV-infected cells were collected 48 hr after infection; cells were trypsinized, resuspended in the tissue culture medium, and subsequently incubated for 1 hr at 37°C to allow recovery of receptor expression on the cell surface. The cell suspension was cooled to 4°C, and equal aliquots were distributed into 1.5-ml tubes. ^{68}Ga-DOTATATE was added at a final concentration of 100 n*M*. The tubes were subsequently incubated at 4°C for 1 hr while rotating. Bound radioactivity was then separated by centrifuging the cells through dibutyl phthalate (Sigma-Aldrich), freezing the tubes on dry ice, and excising the cell pellet-containing tips of the tubes. Bound and free radioactivity was thus determined with a Wallac Wizard gamma counter (Wallac Oy, Turku, Finland) and the number of bound molecules per cell calculated.

Immunofluorescence with anti-hSSTR2 antibodies

Cells fixed in 4% PFA or 12-μm sections from OCT-embedded livers and muscles were permeabilized with 0.1% Triton in PBS for 5 min at room temperature (RT) and incubated overnight in blocking solution (10% FBS, 0.1% bovine serum albumin, 0.1% Triton in PBS). Anti-hSSTR2 antibodies (Affinity Bioreagents, Thermo Scientific, Rockford, IL) were diluted 1:200 in blocking solution, and cells or sections were incubated with the antibody solution for 2 hr at RT. After washing in PBS/0.1% Triton, secondary antibody diluted 1:1,000 in blocking solution was added [fluorescein isothiocyanate (FITC)-labeled anti-rabbit; AlexaFluor, Invitrogen]. Slides were mounted with Vectashield medium (Vector Labs, Burlingame, CA), and pictures were taken under a fluorescence microscope. Magnification of 20×was used for cell and tissue stainings.

Statistical analysis

Data sets in each experiment were analyzed by ANOVA to evaluate statistically significant differences. The Tukey multiple comparison procedure (*post hoc*) was used to make comparisons among groups. Significance at $p \leq 0.05$ is indicated by asterisks in the figures. Correlation between data sets has been evaluated with the Microsoft Excel Pearson test function, and the Pearson product moment correlation coefficient R is reported for each analysis.

Results and Discussion

Generation and in vitro *characterization of AAV vectors expressing hSSTR2*

To assess the applicability of hSSTR2 as a reporter gene for repetitive noninvasive monitoring of AAV-mediated gene transfer, we selected liver and muscle as target tissues for *in vivo* gene delivery, because these are common targets of gene transfer-based therapeutic approaches (Brunetti-Pierri and Auricchio, 2010). SSTR2 endogenous expression is mainly localized to the central nervous system (Yamada *et al.*, 1992; Bruno *et al.*, 1993), and it has been reported also in kidney, pancreas, spleen, and stomach (Yamada *et al.*, 1992; Bruno *et al.*, 1993; Ray *et al.*, 2001), whereas liver and muscle are generally considered negative for SSTR2 expression (Froidevaux *et al.*, 2002), even though low levels of liver SSTR2 expression have been reported (Yamada *et al.*, 1992).

To target the muscle, we generated AAV2/1 vectors bearing the hSSTR2 cds under the control of the ubiquitous cytomegalovirus (CMV) promoter (AAV2/1-CMV-hSSTR2; Fig. 1A, top schematic representation). For liver transduction, we produced AAV2/8 vectors including hSSTR2 under the transcriptional control of the liver-specific thyroxine-binding globulin (TBG) promoter (Ill *et al.*, 1997) (AAV2/8-TBG-hSSTR2; Fig. 1A, bottom schematic representation).

To test AAV-mediated hSSTR2 expression *in vitro* and its dependence on vector dose, we infected 293 cells with

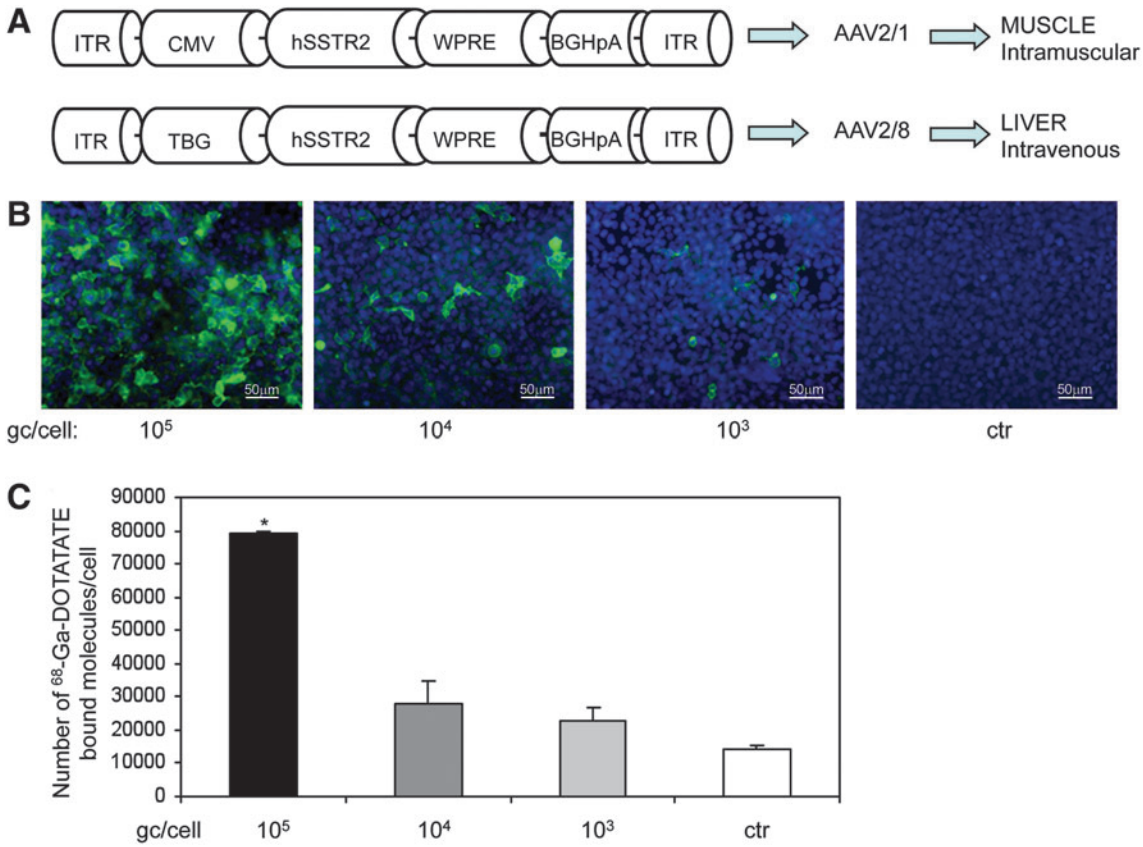

FIG. 1. Schematic representation and *in vitro* expression from AAV vectors encoding hSSTR2. (**A**) Schematic representation of AAV vectors for muscle (*top*) and liver (*bottom*) transduction. In particular, the vectors depicted are AAV2/1-CMV-hSSTR2 (*top*) and AAV2/8-TBG-hSSTR2 (*bottom*), containing the hSSTR2 coding sequence under the control of the ubiquitous CMV (cytomegalovirus enhancer/promoter; *top*) or of the liver-specific TBG (thyroxine-binding globulin; *bottom*) promoter. ITR, AAV inverted terminal repeats; BGHpA, bovine growth hormone polyA; WPRE, woodchuck hepatitis virus posttranscriptional regulatory element; hSSTR2, human somatostatin receptor 2 coding sequence; CMV, cytomegalovirus enhancer/promoter; TBG, thyroxine-binding globulin promoter. (**B**) Dependence of hSSTR2 expression on AAV vector dose in cells transduced *in vitro*. HEK293 cells were infected with the doses of AAV2/1-CMV-hSSTR2 reported under each panel, and anti-SSTR2 immunofluorescence was performed 48 hr later. The fluorescence intensity is proportional to the dose of vector used. ctr, uninfected cells. (**C**) Dependence of ^{68}Ga-DOTATATE binding on AAV vector dose in cells transduced *in vitro*. Binding assays with the SSTR2 ligand ^{68}Ga-DOTATATE were performed on HEK293 cells infected with various doses of AAV2/1-CMV-hSSTR2 (reported under each bar) or with control AAV2/1-CMV-eGFP vectors (ctr; 10^5 gc/cell). Binding of ^{68}Ga-DOTATATE was observed in hSSTR2-expressing cells. The extent of ligand binding was proportional to the AAV vector dose used. Results are from two duplicates and are reported as means $\pm$ SE. $^*p \leq 0.001$ vs. ctr.

various doses of AAV2/1-CMV-hSSTR2 vectors (Fig. 1B and C). Anti-hSSTR2 immunofluorescence analysis showed a direct correlation between the fluorescence intensity of infected cells and the vector doses used ($R = 0.83$). Binding assays performed with ^{68}Ga-DOTATATE showed higher binding levels in cells infected with AAV at higher MOI and showing higher hSSTR2 expression levels than in control cells (Fig. 1C). The binding extent was proportional to the AAV vector dose used ($R = 0.99$) and to the amount of hSSTR2 expressed (fluorescence intensity) in infected cells ($R = 0.79$).

Noninvasive, repetitive monitoring of hSSTR2 expression in liver and muscle transduced with AAV

To assess hSSTR2 expression *in vivo*, we injected 4-week-old C57bl/6 mice with 1×10^{11} gc of either AAV2/1 or AAV2/8 vectors in the right gastrocnemius or in the tail vein, respectively. Six months after vector delivery, mice were sacrificed, transduced livers and muscles were harvested, and hSSTR2 expression was assessed by immunofluorescence (Supplementary Fig. S1; supplementary data are available online at www.liebertonline.com/hum). As expected, the anti-hSSTR2 staining showed a signal consistent with membrane localization of the transgene product in both tissues. Immunofluorescence analysis performed on liver and muscle sections from control uninjected mice showed no specific SSTR2 signal, suggesting that, as already reported, endogenous SSTR2 is expressed at undetectable levels in murine liver and muscle (Froidevaux *et al.*, 2002) (Supplementary Fig. S1).

After obtaining efficient AAV-mediated hSSTR2 transgene expression in the murine liver and muscle, we tested the possibility of noninvasively monitoring its expression by PET. Four-week-old C57bl/6 mice were injected with 1×10^{11}

gc of either AAV2/1-CMV-hSSTR2 or AAV2/8-TBG-hSSTR2 vectors in the right gastrocnemius or in the tail vein, respectively. Control mice received the same dose of AAV2/1-CMV-eGFP, AAV2/1-CMV-LacZ, AAV2/8-TBG-eGFP, or AAV2/8-TBG-LacZ vectors. Four weeks after vector delivery, mice were injected with 1–6 MBq of ^{68}Ga-DOTATATE via the tail vein and subjected to PET-CT scan for localization of the radiotracer signal.

Control mice, whether uninjected or injected with AAV systemically or intramuscularly, showed a positive signal in the kidneys (Fig. 2A, bottom picture, green arrowhead) and bladder (Fig. 2A, bottom picture, white arrowhead). This is consistent with DOTATATE urinary excretion, as previously described (Froidevaux *et al.*, 2002), or with ^{68}Ga-DOTATATE potential binding to other SSTR subtypes endogenously expressed in the kidney (Yamada *et al.*, 1992; Hoyer *et al.*, 1995). In our experimental conditions, control mice did not show a significant PET signal in either muscle or liver (Fig. 2A, bottom picture), confirming the suitability of hSSTR2 as a reporter gene for *in vivo* imaging of gene transfer in these tissues.

In contrast, we observed a strong signal in the liver of mice injected with AAV2/8-TBG-hSSTR2 vectors (Fig. 2A, top picture, arrow); mice receiving intramuscular injection of AAV2/1-CMV-hSSTR2 vectors, moreover, showed a positive signal specifically localized to the right injected leg (Fig. 2A, middle picture, arrow). The stronger bladder signal that was evident in mice transduced in muscle (Fig. 2A, middle picture, white arrowhead) compared with those transduced in liver (Fig. 2A, top picture, white arrowhead) is mostly due to the uptake threshold value selected for the images, which is lower for muscle than for liver. In addition, the amount of tracer being excreted from the bladder may reflect the lower specific ^{68}Ga-DOTATATE uptake in animals transduced in muscle than in the liver.

To obtain quantitative assessment of radiotracer accumulation in muscle and liver transduced with AAV, we measured the %ID/g in regions showing a significant PET signal. The %ID/g was multiplied by the volume of the region analyzed (%ID/g×V) for comparisons. As control, %ID/g×V was measured in the same regions of mice receiving AAV-eGFP or AAV-LacZ vectors or of uninjected mice. The %ID/g×V values measured in either the liver (Fig. 2B, top panel, black bar) or muscle (Fig. 2B, bottom panel, black bar) transduced with AAV were significantly higher than in the corresponding regions of control mice (Fig. 2B, "ctr" bars).

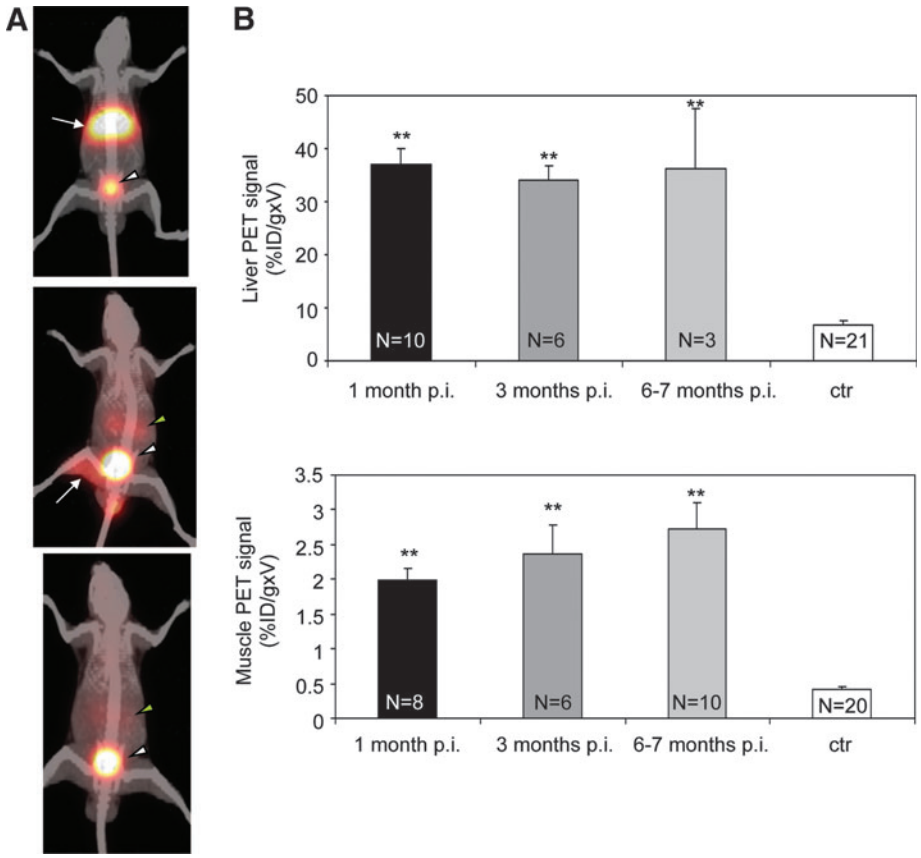

FIG. 2. PET imaging of murine liver and muscle administered with AAV: long-term, repeated detection of hSSTR2 expression. (**A**) *In vivo* imaging of hSSTR2 expression in AAV-injected mice. Adult C57bl/6 mice were injected either systemically with AAV2/8-TBG-hSSTR2 (*top picture*) or intramuscularly with AAV2/1-CMV-hSSTR2 (*middle picture*). A control animal received AAV2/8-TBG-LacZ systemically (*bottom picture*). PET-CT imaging of hSSTR2 was performed following systemic administration of ^{68}Ga-DOTATATE 1 month after AAV delivery. Representative pictures of animals from each group are shown. Specific tracer uptake is observed in the liver (*top picture*, white arrow) or in the muscle (*middle picture*, white arrow) of mice treated with AAV2/8-TBG-hSSTR2 or AAV2/1-CMV-hSSTR2, respectively. Control mice (*bottom picture*) show a nonspecific uptake in kidneys (green arrowhead) and bladder (white arrowhead), representing the ^{68}Ga-DOTATATE route of excretion. PET images are windowed to a fixed %ID/g threshold value of 25 for animals receiving AAV intravenously and control mice, and 15 for animals receiving AAV intramuscularly. (**B**) Quantitative repetitive measurement of ^{68}Ga-DOTATATE binding in transduced tissues. PET imaging of SSTR2 expression was performed following systemic administration of ^{68}Ga-DOTATATE 1, 3, and 6 months after AAV delivery, and the %ID/g×V was measured. The bar labeled "ctr" corresponds to control mice uninjected or injected with AAV2/1-CMV-eGFP, AAV2/1-CMV-LacZ, AAV2/8-TBG-eGFP, or AAV2/8-TBG-LacZ vectors. The %ID/g×V values for liver (*top*) and muscle (*bottom*) are shown. Results are reported as means ± SE. The number of animals analyzed for each group is reported in the corresponding column. $^{**}p < 0.001$ vs. ctr. p.i., post injection.

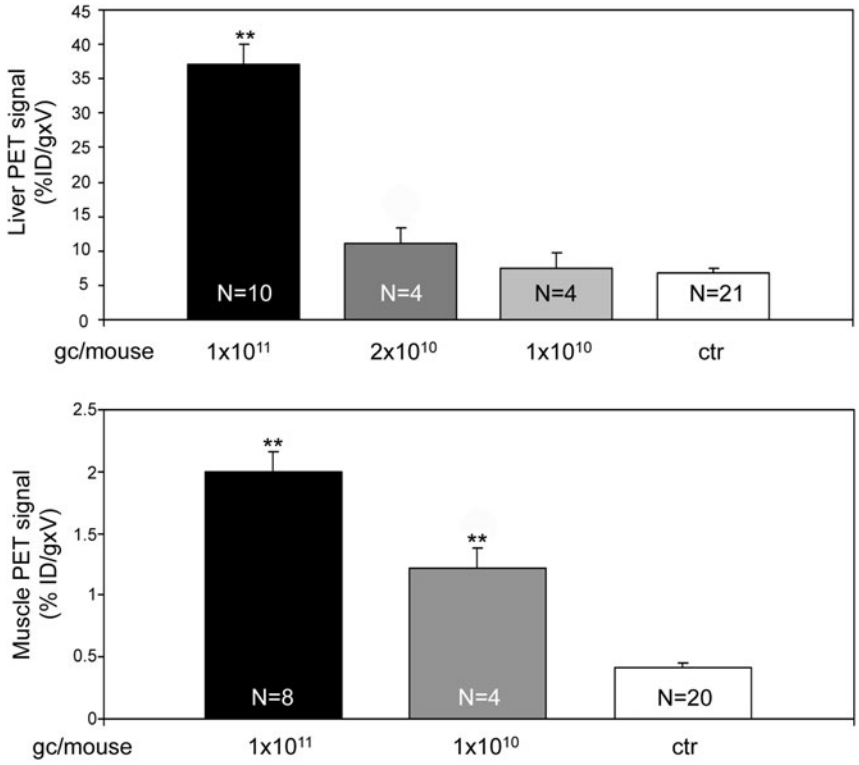

FIG. 3. Dependence of ^{68}Ga-DOTATATE uptake on AAV dose in transduced murine liver and muscle. One-month-old C57bl/6 mice were injected systemically with AAV2/8-TBG-hSSTR2 (*top panel*) or intramuscularly with AAV2/1-CMV-hSSTR2 (*bottom panel*) at the vector doses reported under each bar. As control (ctr), animals received 1×10^{11} gc of AAV2/1-CMV-eGFP, AAV2/1-CMV-LacZ, AAV2/8-TBG-eGFP, or AAV2/8-TBG-LacZ vectors. PET imaging of SSTR2 was performed 1 month after AAV delivery, and the %ID/g×V was calculated and reported. Results are reported as means ± SE. $^{**}p \leq 0.001$ vs. ctr. The number of animals analyzed in each group is reported in the corresponding bar.

To monitor long-term hSSTR2 transgene expression, we repeated PET analysis on injected animals 3 and 6 months after AAV vector administration. Similar %ID/g×V values were measured in both the liver and muscle at all time points tested, confirming that PET imaging of hSSTR2 reporter transgene allows long-term repetitive and quantitative imaging of tissue transduction. Although all animals injected with AAV in the muscle showed persistence of hSSTR2 transgene expression and of high %ID/g×V values, some of the mice transduced in the liver (see the number of animals reported on each bar in Fig. 2B, top panel) lost both hSSTR2 expression and PET signal between 3 and 6 months after AAV administration, resulting in %ID/g×V values similar to those measured in control animals. We hypothesized that this could be due to immune responses to the vector or to the hSSTR2 transgene expressed by transduced murine liver cells. Indeed PET analysis showed higher signal in liver than muscle (Fig. 2A and B). To test this hypothesis, immunodeficient BalbC nude mice were systemically injected with 1×10^{11} gc of AAV2/8-TBG-hSSTR2 vectors, and PET analysis was performed 1, 3, and 6 months after vector delivery. All injected nude mice showed persistence of the %ID/g×V values until the last time point analyzed (Supplementary Fig. S2), suggesting that the loss of transgene expression observed in some immunocompetent C57bl/6 mice may be due to immuno-mediated clearance of hSSTR2-expressing cells. Alternatively, strain-dependent differences in AAV-mediated liver transduction may result in hSSTR2 overexpression and toxicity, leading to loss of PET signal in C57bl/6 mice.

An ideal system for noninvasive quantitative measurement of gene transfer should provide a signal that is dependent on the levels of transgene expressed. To test this hypothesis, we injected C57bl/6 mice with various doses of AAV2/8-TBG-hSSTR2 (Fig. 3, top panel) or AAV2/1-CMV-hSSTR2 (Fig. 3, bottom panel). PET scans were performed 1 month after vector delivery on injected and control mice, and %ID/g×V values were measured. In animals transduced in the liver, we observed a specific ^{68}Ga-DOTATATE signal in mice receiving 1×10^{11} and 2×10^{10} vector gc, whereas in mice injected with 1×10^{10}gc, the PET signal was undistinguishable from the background observed in control animals (data not shown). Consistent with this, the %ID/g×V was increased over background only in mice receiving 1×10^{11} and 2×10^{10} gc and was proportional to the AAV vector dose injected ($R = 0.99$; Fig. 3, top panel). Thus, 2×10^{10} gc/mouse is the lowest dose resulting in hSSTR2 transgene expression detectable by PET in the liver. Use of microPET may allow the detection of lower transgene expression levels. In mice receiving AAV intramuscularly, a specific PET signal was observed in all animals administered 1×10^{11}gc/mouse and 1×10^{10}gc/mouse, with the corresponding %ID/g×V directly correlating with the AAV vector dose injected ($R = 0.9$; Fig. 3, bottom panel).

In conclusion, our data indicate that the AAV-hSSTR2/^{68}Ga-DOTATATE system has the potential for efficient, repetitive, and quantitative PET-mediated monitoring of gene delivery *in vitro* and *in vivo* in common gene transfer target tissues, such as the liver or muscle. This supports the use of hSSTR2 as reporter gene to be either coexpressed with a therapeutic transgene to infer its location and levels of expression, or as a tool to optimize transduction levels, specificity, and duration of transgene expression in gene therapy protocols.

Acknowledgments

We are grateful to Luciana Borrelli and Graciana Diez-Roux for critically reviewing the manuscript. We thank the TIGEM AAV Vector Core for the production of the AAV vectors used in this study and the TIGEM Bioinformatics Core for the statistical analysis of the data reported in this article. This work was supported by the Telethon Grant TIGEM P33, DiMI, and 018933 Clinigene from the European Community and by the European Commission under the FP7 Euclyd project (grant no. HEALTH-F2-2008-201678).

Author Disclosure Statement

The authors declare no conflicts of interest.

References

Auricchio, A., Hildinger, M., O'Connor, E., Gao, G.P., and Wilson, J.M. (2001). Isolation of highly infectious and pure adeno-associated virus type 2 vectors with a single-step gravity-flow column. Hum. Gene Ther. 12, 71–76.

Brunetti-Pierri, N., and Auricchio, A. (2010). Gene therapy of human inherited diseases. In *The Online Metabolic and Molecular Bases of Inherited Diseases*. Valle, Beaudet, Vogelstein, Kinzler, Antonarakis, and Ballabio, eds. Available at http://www.ommbid.com/OMMBID/the_online_metabolic_and_molecular_bases_of_inherited_disease/b/abstract/part2/ch5.2. Accessed December 13, 2010.

Bruno, J.F., Xu, Y., Song, J., and Berelowitz, M. (1993). Tissue distribution of somatostatin receptor subtype messenger ribonucleic acid in the rat. Endocrinology 133, 2561–2567.

Froidevaux, S., Eberle, A.N., Christe, M., Sumanovski, L., Heppeler, A., Schmitt, J.S., Eisenwiener, K., Beglinger, C., and Macke, H.R. (2002). Neuroendocrine tumor targeting: study of novel gallium-labeled somatostatin radiopeptides in a rat pancreatic tumor model. Int. J. Cancer 98, 930–937.

Gambhir, S.S., Bauer, E., Black, M.E., Liang, Q., Kokoris, M.S., Barrio, J.R., Iyer, M., Namavari, M., Phelps, M.E., and Herschman, H.R. (2000a). A mutant herpes simplex virus type 1 thymidine kinase reporter gene shows improved sensitivity for imaging reporter gene expression with positron emission tomography. Proc. Natl. Acad. Sci. U.S.A. 97, 2785–2790.

Gambhir, S.S., Herschman, H.R., Cherry, S.R., Barrio, J.R., Satyamurthy, N., Toyokuni, T., Phelps, M.E., Larson, S.M., Balatoni, J., Finn, R., Sadelain, M., Tjuvajev, J., and Blasberg, R. (2000b). Imaging transgene expression with radionuclide imaging technologies. Neoplasia 2, 118–138.

Gao, G., Qu, G., Burnham, M.S., Huang, J., Chirmule, N., Joshi, B., Yu, Q.C., Marsh, J.A., Conceicao, C.M., and Wilson, J.M. (2000). Purification of recombinant adeno-associated virus vectors by column chromatography and its performance *in vivo*. Hum. Gene Ther. 11, 2079–2091.

Gilad, A.A., Ziv, K., McMahon, M.T., Van Zijl, P.C., Neeman, M., and Bulte, J.W. (2008). MRI reporter genes. J. Nucl. Med. 49, 1905–1908.

Groot-Wassink, T., Aboagye, E.O., Wang, Y., Lemoine, N.R., Reader, A.J., and Vassaux, G. (2004). Quantitative imaging of Na/I symporter transgene expression using positron emission tomography in the living animal. Mol. Ther. 9, 436–442.

Herzog, H., Coenen, H.H., Kuwert, T., Langen, K.J., and Feinendegen, L.E. (1990). Quantification of the whole-body distribution of PET radiopharmaceuticals, applied to 3-*N*-([^{18}F]fluoroethyl)spiperone. Eur. J. Nucl. Med. 16, 77–83.

Hofland, L.J., and Lamberts, S.W. (1996). Somatostatin receptors and disease: role of receptor subtypes. Baillieres Clin. Endocrinol. Metab. 10, 163–176.

Hoyer, D., Bell, G.I., Berelowitz, M., Epelbaum, J., Feniuk, W., Humphrey, P.P., O'Carroll, A.M., Patel, Y.C., Schonbrunn, A., Taylor, J.E., *et al*. (1995). Classification and nomenclature of somatostatin receptors. Trends Pharmacol. Sci. 16, 86–88.

Ill, C.R., Yang, C.Q., Bidlingmaier, S.M., Gonzales, J.N., Burns, D.S., Bartholomew, R.M., and Scuderi, P. (1997). Optimization of the human factor VIII complementary DNA expression plasmid for gene therapy of hemophilia A. Blood Coagul. Fibrinolysis 8 Suppl 2, S23–S30.

Jiang, H., Pierce, G.F., Ozelo, M.C., De Paula, E.V., Vargas, J.A., Smith, P., Sommer, J., Luk, A., Manno, C.S., High, K.A., and Arruda, V.R. (2006). Evidence of multiyear factor IX expression by AAV-mediated gene transfer to skeletal muscle in an individual with severe hemophilia B. Mol. Ther. 14, 452–455.

Kayani, I., Bomanji, J.B., Groves, A., Conway, G., Gacinovic, S., Win, T., Dickson, J., Caplin, M., and Ell, P.J. (2008). Functional imaging of neuroendocrine tumors with combined PET/CT using ^{68}Ga-DOTATATE (DOTA-DPhe1,Tyr3-octreotate) and ^{18}F-FDG. Cancer 112, 2447–2455.

Kundra, V., Mannting, F., Jones, A.G., and Kassis, A.I. (2002). Noninvasive monitoring of somatostatin receptor type 2 chimeric gene transfer. J. Nucl. Med. 43, 406–412.

MacLaren, D.C., Gambhir, S.S., Satyamurthy, N., Barrio, J.R., Sharfstein, S., Toyokuni, T., Wu, L., Berk, A.J., Cherry, S.R., Phelps, M.E., and Herschman, H.R. (1999). Repetitive, non-invasive imaging of the dopamine D2 receptor as a reporter gene in living animals. Gene Ther. 6, 785–791.

Manno, C.S., Chew, A.J., Hutchison, S., Larson, P.J., Herzog, R.W., Arruda, V.R., Tai, S.J., Ragni, M.V., Thompson, A., Ozelo, M., Couto, L.B., Leonard, D.G., Johnson, F.A., McClelland, A., Scallan, C., Skarsgard, E., Flake, A.W., Kay, M.A., High, K.A., and Glader, B. (2003). AAV-mediated factor IX gene transfer to skeletal muscle in patients with severe hemophilia B. Blood 101, 2963–2972.

Miederer, M., Seidl, S., Buck, A., Scheidhauer, K., Wester, H.J., Schwaiger, M., and Perren, A. (2009). Correlation of immunohistopathological expression of somatostatin receptor 2 with standardised uptake values in ^{68}Ga-DOTATOC PET/CT. Eur. J. Nucl. Med. Mol. Imaging 36, 48–52.

Min, J.J., and Gambhir, S.S. (2008). Molecular imaging of PET reporter gene expression. Handb. Exp. Pharmacol. 185 Part 2, 277–303.

Ray, P., Bauer, E., Iyer, M., Barrio, J.R., Satyamurthy, N., Phelps, M.E., Herschman, H.R., and Gambhir, S.S. (2001). Monitoring gene therapy with reporter gene imaging. Semin. Nucl. Med. 31, 312–320.

Rogers, B.E., Zinn, K.R., Lin, C.Y., Chaudhuri, T.R., and Buchsbaum, D.J. (2002). Targeted radiotherapy with [^{90}Y]-SMT 487 in mice bearing human nonsmall cell lung tumor xenografts induced to express human somatostatin receptor subtype 2 with an adenoviral vector. Cancer 94, 1298–1305.

Rogers, B.E., Chaudhuri, T.R., Reynolds, P.N., Della Manna, D., and Zinn, K.R. (2003). Non-invasive gamma camera imaging of gene transfer using an adenoviral vector encoding an epitope-tagged receptor as a reporter. Gene Ther. 10, 105–114.

Rogers, B.E., Parry, J.J., Andrews, R., Cordopatis, P., Nock, B.A., and Maina, T. (2005). MicroPET imaging of gene transfer with a somatostatin receptor-based reporter gene and ^{94m}Tc-Demotate 1. J. Nucl. Med. 46, 1889–1897.

Singh, S.P., Yang, D., Ravoori, M., Han, L., and Kundra, V. (2009). In vivo functional and anatomic imaging for

assessment of in vivo gene transfer. Radiology 252, 763–771.

Win, Z., Al-Nahhas, A., Towey, D., Todd, J.F., Rubello, D., Lewington, V., and Gishen, P. (2007). ^{68}Ga-DOTATATE PET in neuroectodermal tumours: first experience. Nucl. Med. Commun. 28, 359–363.

Xiao, W., Chirmule, N., Berta, S.C., McCullough, B., Gao, G., and Wilson, J.M. (1999). Gene therapy vectors based on adeno-associated virus type 1. J. Virol. 73, 3994–4003.

Yamada, Y., Post, S.R., Wang, K., Tager, H.S., Bell, G.I., and Seino, S. (1992). Cloning and functional characterization of a family of human and mouse somatostatin receptors expressed in brain, gastrointestinal tract, and kidney. Proc. Natl. Acad. Sci. U.S.A. 89, 251–255.

Zinn, K.R., and Chaudhuri, T.R. (2002). The type 2 human somatostatin receptor as a platform for reporter gene imaging. Eur. J. Nucl. Med. Mol. Imaging 29, 388–399.

Zinn, K.R., Buchsbaum, D.J., Chaudhuri, T.R., Mountz, J.M., Grizzle, W.E., and Rogers, B.E. (2000). Noninvasive monitoring of gene transfer using a reporter receptor imaged with a high-affinity peptide radiolabeled with ^{99m}Tc or ^{188}Re. J. Nucl. Med. 41, 887–895.

Zinn, K.R., Chaudhuri, T.R., Krasnykh, V.N., Buchsbaum, D.J., Belousova, N., Grizzle, W.E., Curiel, D.T., and Rogers, B.E. (2002). Gamma camera dual imaging with a somatostatin receptor and thymidine kinase after gene transfer with a bicistronic adenovirus in mice. Radiology 223, 417–425.

Address correspondence to:
Dr. Alberto Auricchio
Department of Pediatrics, "Federico II" University, Naples
Principal Investigator
Telethon Institute of Genetics and Medicine (TIGEM)
Via P. Castellino 111
80131 Naples
Italy

Email: auricchio@tigem.it

Dr. Luigi Aloj
Nuclear Medicine
Istituto Nazionale per lo Studio e la Cura dei Tumori
Fondazione "G. Pascale"
Via M. Semmola
80131, Naples
Italy

E-mail: luigi.aloj@fondazionepascale.it

Received for publication May 11, 2010;
accepted after revision September 7, 2010.

Published online: September 8, 2010.